Journal of Applied Polymer Science

Polyurethane/organic vermiculite composites with enhanced mechanical properties

Tailiang Zhang, Fangjie Zhang, Shanshan Dai, Zefeng Li, Baogang Wang, Hongping Quan, Zhiyu Huang

School of Chemistry and Chemical Engineering, Southwest Petroleum University, Chengdu 610500, People's Republic of China
Correspondence to: S. Dai (E-mail: ashanscu@163.com)

ABSTRACT: In this article, a series of polyurethane (PU)/organic vermiculite (OVMT) composites are prepared by intercalating polymerization. 1,4-cyclohexane diisocyanate (CHDI) as hard segment of PU is designed to improve the decomposition temperature of composites. Vermiculite (VMT) is modified by method of cation exchange with octadecyl trimethyl ammonium bromide (OTAB); the resulting product OVMT with the function of physical cross-linking disperses well in soft segment of PU polycarbonate polyol (PCDL), which improves the mechanical properties of composites obviously. This modification further enlarged the interlayer of OVMT and improved the properties of composites. The structure and properties of OVMT and PU/OVMT composites are characterized by Fourier transform infrared spectroscopy, X-ray diffraction, thermogravimetric analysis, scanning electron microscope, and tensile strength test. The results showed that the layer spacing of OVMT increased 1.41 nm compared with that of VMT (the value of layer spacing of VMT is 0.96 nm) and further enlarged to 2.92 nm by the loading of PCDL. The tensile strength and the strain at break of PUCPB/OVMT (3.0%) composites reached 26.8 MPa and 443%, respectively. The temperature resistance of PUCPB/OVMT (3.0%) composites is above 300°C, which is more suitable for the steam channeling plugging of heavy oil. © 2015 Wiley Periodicals, Inc. J. Appl. Polym. Sci. **2016**, *133*, 43219.

KEYWORDS: composites; functionalization of polymers; oil and gas; X-ray

Received 18 June 2015; accepted 10 November 2015
DOI: 10.1002/app.43219

INTRODUCTION

Polyurethane (PU) is one of the most versatile materials because of some unique properties. It has received much attention on the study of its synthesis, morphology, chemical, or mechanical properties.[1,2] Today, PU is widely used in coatings, adhesives, binders, paints, thermoplastic elastomers, composites, and so on.

Properties of PU can be adjusted by two approaches: first, modification of three basic building blocks: polyether or polyester, diisocyanate, and chain extender to control the molecule structure of PU; second, loading of inorganic fillers into the PU matrix. It has been found possible to improve many properties of PU by incorporating fillers.[1]

Vermiculite (VMT) as a special kind of layered silicate minerals is composed of tetrahedral and octahedral sheets, which provides high cation exchange and adsorption capacity. In addition, metal cations, such as hydrated Mg^{2+}/Al^{3+} in natural VMT, are located between the layers to balance the charge. Water molecules associated with internal surfaces evokes hydration of interlayer cations.[3]

In order to improve the performance of the VMT and make the polymer easily into the interlayer, VMT is modified by intercalating organic reagents.[4,5] The principle of ion exchange is used to make the organic cation into silicate lamella, to expand the layer spacing, and to improve the interlayer microenvironment.[6–8] It made the surface of VMT class clay from hydrophilic into hydrophobic, enhances the affinity between the lamella and polymer molecular chain, and also can reduce the surface energy of silicate material, which lead it easier to insert the polymer monomer or molecular chain.[9–11]

PU/silicate composites have excellent comprehensive properties, such as high strength and resistant temperature. It is widely used in petroleum, coal, and many other industries.[1,12–14] The addition of inorganic materials to the PU is an important way to improve the heat-resistant properties of PU. Composites are prepared by intercalating polymerization of inorganic and organic phases.[15–19] Much of its performance is superior compared with conventional composites, such as mechanical properties,[20,21] thermal properties,[22,23] water absorption performance, and so on.

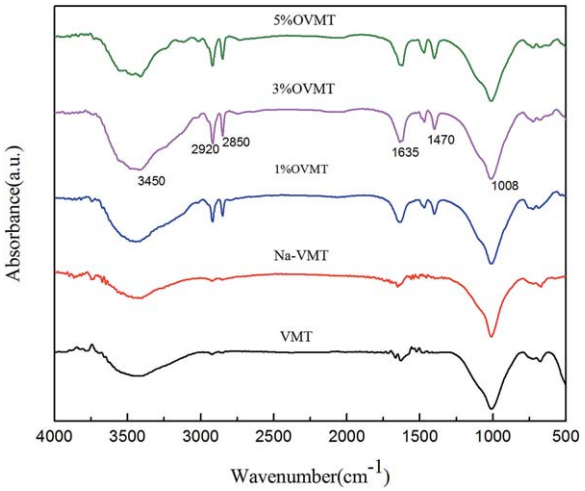

Figure 1. FT-IR spectra of VMT and OVMT. [Color figure can be viewed in the online issue, which is available at wileyonlinelibrary.com.]

Most of the PU is applied in waterproof, adhesive, thermal insulation, and so on. Its application in plugging steam channeling of heavy oil reservoirs is rarely reported. Usually, plugging agents have high initial viscosity and instability in high temperature, such as ethoxyline resin and sulfonated polymer. PU is easy to pump due to the low initial viscosity and it can react with water into an expansion, which can improve the thermal properties and avoid the shortcoming of ethoxyline resin and sulfonated polymer. The addition of VMT can further increase the compressive strength of composites, which is more suitable for the application in steam huff-puff.

In this article, octadecyl trimethyl ammonium bromide (OTAB) as intercalating agent is used to modify VMT. 1,4-cyclohexane diisocyanate as hard segment and polycarbonate polyol as soft segment prepared the PU/organic vermiculite (OVMT) composites by intercalating polymerization. The influence factor of layer spacing of VMT is researched and the performance of composites is discussed.

EXPERIMENTAL SECTION

Materials

VMT (cation exchange capacity (CEC) = 119.0 mmol/100 g), sodium chloride, OTAB (^{18}C, 99%, Sigma), 1,4-cyclohexane diisocyanate (CHDI, 98%, Sigma), and polycarbonate polyol (PCDL, M_n = 2000 g/mol), which obtained in the Wanhua group of Shandong Province (BDO, 99%, Sigma), were dried before use.

Organic Modified Vermiculite

The VMT was modified as follows: VMT powder (10 g) was dispersed in 100 mL of 6.0% NaCl solution and the mixture was refluxed for 2 h at 70°C. The product was separated by centrifugation and washed several times with deionized water, then dried for 2 h in a vacuum oven at 110°C to form Na-VMT. The OVMT was synthesized by exchanging Na-VMT with OTAB ^{4}.66 g/13.98 g/23.30 g (the effective cation exchange capacity (CEC = 119.0 mmol/100 g)), at 75°C for 2 h. The product was separated by centrifugation, washed several times with deionized water, and then dried for 2 h in a vacuum oven at 110°C. The OVMT was denoted OTAB–VMT (OVMT).

Preparation of PUCPB/OVMT Composites

PCDL was dried for 2 h at 110°C in the vacuum oven before use. Different concentrations of OVMT were added to the polycarbonate polyol to form dispersions with 0.0, 1.0, 3.0, 5.0, or 7.0 wt %. The mixtures were stirred at 1000 rpm for 2 h and then subjected to ultrasonic processor for 2 h. CHDI (4.98 g) was added at 75°C for 0.5 h, with 2*n*-butyl amine method – NCO content after reaching the theoretical value, then cooled to 70°C, 1.35 g BDO was added for 1 h, then under vacuum for 30 min, and then poured into a mold into the vacuum drying oven at 110°C curing for 4 h. The polymer was cured at room temperature for 7 days after test. The resulting composites were denoted as PUCPB/OVMT(x) (x is the OVMT weight percentage).

Characterization

Fourier transform-infrared (FT-IR) spectroscopy was carried out using a WQF-520 spectrometer, and the pellet sample was prepared by pressing the mixture of the compatibilizer and KBr powder.

X-ray diffraction (XRD) patterns were acquired using a PANalytical X-Pert Pro X-ray diffractometer equipped with a Co source (40 kV, 30 mA, λ = 1.790 Å) and an X-Celerator detector. X-ray scattering patterns of PU composites were acquired on a PANalytical X-Pert Pro X-ray diffractometer instrument with a Cu X-ray source (40 kV, 30 mA).

Thermogravimetric analyses (TGAs) were carried out with an STA449F3-type synchronous comprehensive thermal analyzer in air for the modified VMT and the PU composites, using a ramping rate of 20°C/min.

Environmental scanning electron microscope (SEM) images were obtained on a Quanta450 microscope to fracture morphology analysis of the sample.

Transmission electron microscope (TEM) images were obtained on a JEM-2100 microscope to fracture the dispersion of the OVMT in the PU matrix at 200 kV and 12,000×, 50,000×, and 120,000× magnifications.

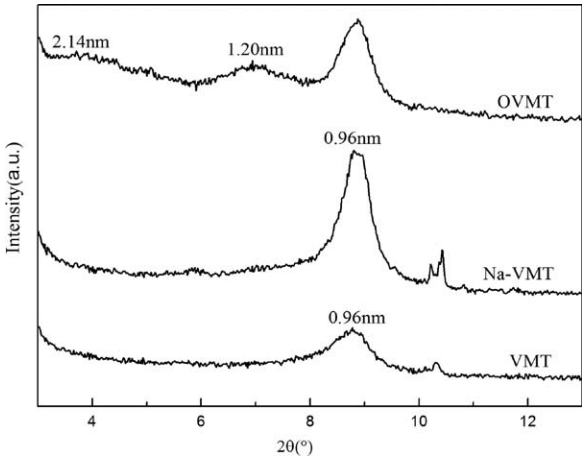

Figure 2. XRD results of vermiculite before and after modified.

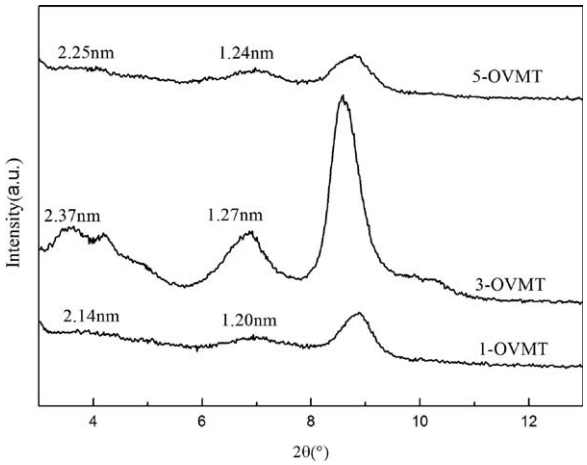

Figure 3. XRD results of OVMT.

Ultimate tensile strength and the hysteresis were measured on a Rheometric Scientific Minimat using dumbbell-shaped samples at 100% strain per second. The samples were prepared according to the GB_T528_1998 and GB_T513_1999.

RESULTS AND DISCUSSION

Modification of VMT

FT-IR Spectra of OVMT. The structure of VMT and OVMT were measured by FT-IR as shown in Figure 1. The pure VMT gave rise to characteristic peaks at 3450 and 1008 cm^{-1}. The peak at 3450 cm^{-1} is related to –OH stretching. The Si−O stretching appeared at 1008 cm^{-1}. Along with the characteristic peaks of VMT, the Na-VMT take little change, new peaks appeared in the FT-IR spectrograph of OVMT. The appearance of two peaks at 2950 and 2850 cm^{-1} is related to C−H symmetric and asymmetric stretching of methyl ($-CH_3$) and methylene ($-CH_2$) group, respectively. The band at 1470 cm^{-1} is assigned to the ammonium salt (N^+–CH_3). Thus, FT-IR spectra revealed that the characteristic peak of OTAB is obvious.

Figure 1 shows the FT-IR spectra of the OVMT films with different concentrations of OTAB. The absorption peak at 3445cm^{-1} is attributed to the –OH of the adsorption water of VMT surface and the layers stretching absorbance. The characteristic stretching peaks of CH_3 and CH_2 occur at 2920 and 2850 cm^{-1}, respectively. The relevant FT-IR bands corresponded to O–H stretching at 1635 cm^{-1} and N^+–CH_3 stretching at 1470 cm^{-1}. The Si−O stretching and Si−O−Si bending vibrations appeared at 1008 and 458 cm^{-1}. The result shows that the different concentrations of OTAB can be intercalated to modify VMT.

XRD Analysis of OVMT. Figure 2 represents the XRD patterns of VMT, Na-VMT, and OVMT. The pure VMT shows the characteristic peak at 2θ of 8.84°, corresponding to the gallery height (d_{001} spacing) of 0.96 nm, while Na-VMT shows the same major peak at 0.96 nm. While OVMT added two new diffraction peaks obviously, incorporation of alkyl quaternary ammonium salts generates a d-spacing of 2.14 nm for OVMT. OVMT shows a weaker peak at d = 1.20 nm, the rather weak and broad diffraction peaks appearing in the XRD curve of ground VMT are attributed to the nonuniform layer spacing between the silicates in VMT and the mono- and double-hydrated Mg^{2+} forms. This result led us to assume that the increase in d_{001} spacing of the OVMT is due to the OTAB inside the interlayer during the ion-exchange reaction.

As shown in Figure 3, XRD patterns were used to investigate the intercalation of VMT interlayer through organic

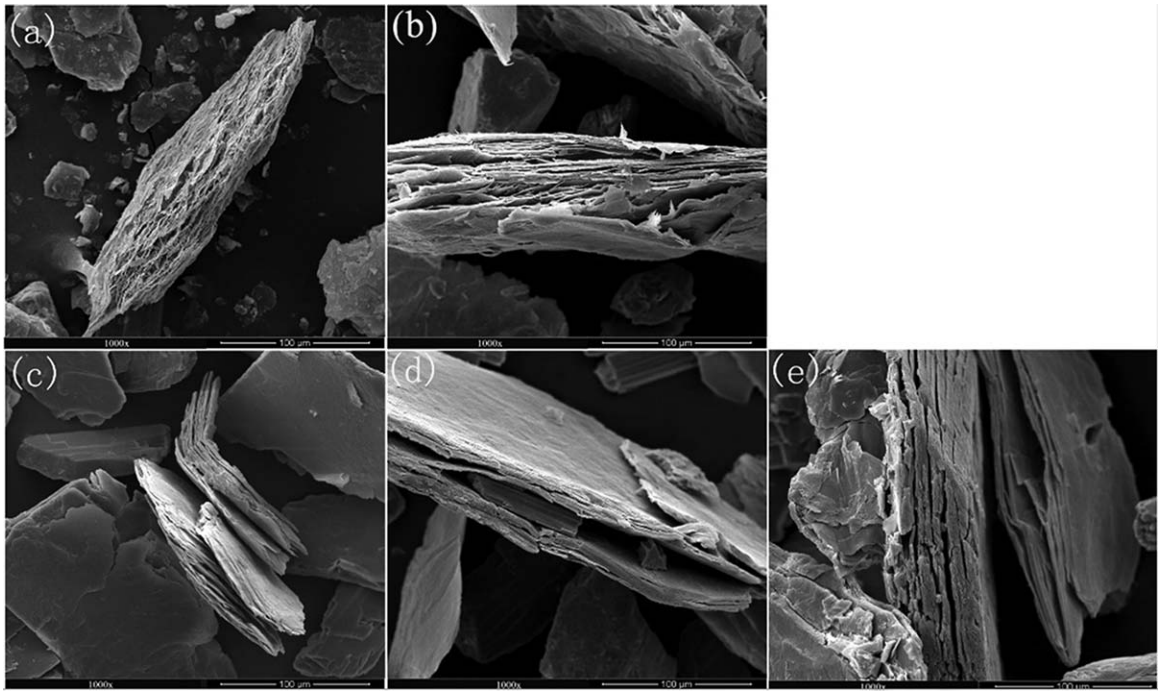

Figure 4. SEM image of (a) VMT, (b) Na-VMT, (c) 1-OVMT, (d) 3-OVMT, and (e) 5-OVMT.

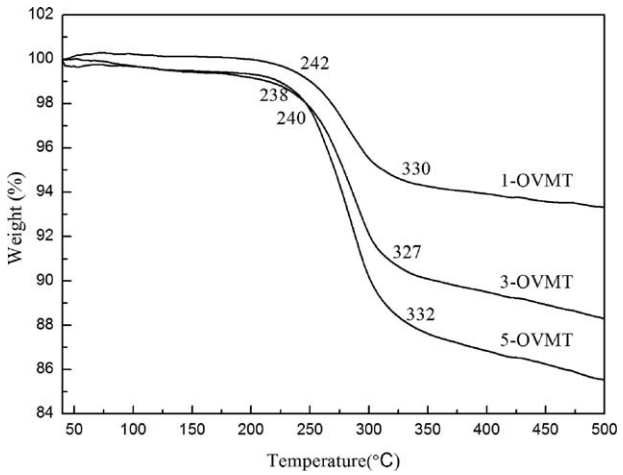

Figure 5. The curves of TGA of OVMT.

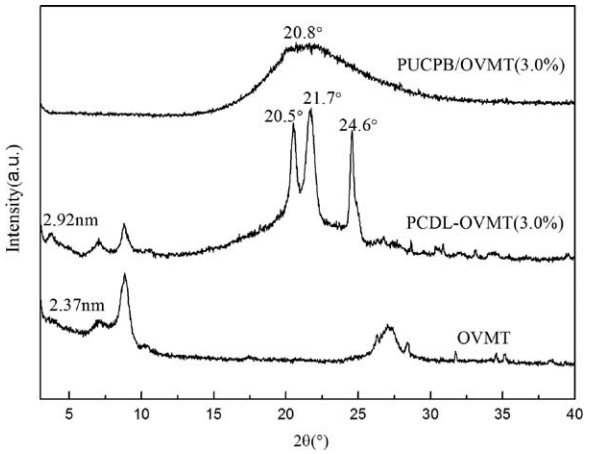

Figure 7. XRD patterns of OVMT, PCDL–OVMT (3.0%), and PUCPB/OMT (3.0%).

modification by different multiples OTAB. It can be seen that the d_{001} peak for the OVMT is shifted to a lower region with the increment of OTAB. [3]-OVMT shows a major broad peak at d = 2.34 nm and a shoulder peak at d = 1.27 nm; 5-OVMT shows a major broad peak at d = 2.25 nm and a shoulder peak at d = 1.20 nm. The layer spacing changes little when the exchange capacity reaches a certain value, which proves that interlayer cations have been exchanged completely. The result shows that 3-OVMT is the best.

SEM Analysis of OVMT. Figure 4 represents the SEM micrographs of the OVMT. As can be seen, the SEM images show the change in the interlayer spacing of VMT and OVMT. The layer spacing of VMT is limited in intercalating polymerization [Figure 4(a)]. In the sodium of modified VMT [Figure 4(b)], other cations of VMT interlayer are replaced by sodium ion, irrespective of the method of composite formation, the lamellar structure of Na-VMT is obvious, and the texture is clear. In Figure 4(c–e), for different added concentrations of OVMT, we can see clearly that the layer spacing of VMT is stretched and increased. 1-OVMT shows in Figure 4(c)) that VMT interlayer is separated and even layer of some pieces have been stripped; Figure 4(d) is the 3-OVMT, in which layer spacing of modified VMT increased obviously and surfactant is embedded in between the layers. Figure 4(e) shows the picture of 5-OVMT, layer spacing is matching with Figure 4(d). The result shows that a new material is intercalated into interlayer of VMT from Figure 4(d,e), so we can judge that OTAB entered the interlayer of VMT and the layer spacing is enlarged, which provide excellent space for the intercalating polymerization.

Thermal Properties Analysis of OVMT. The thermal property of OVMT is evaluated by the TGAs. The thermal decomposition expressed in terms of weight loss as a function of temperature for OVMT is shown in Figure 5. Usually, the total weight loss of VMT is about 3%, which could be attributed to the surface and interlayer absorbed water. The decomposition temperature of OTAB is between 180 and 320°C.[24] The initial decomposition temperature of 3-OVMT is 238°C; a strong exothermic peak shows the structure fracture of OTAB. The corresponding temperature of maximum weight loss rate in this phase is 285°C when it reaches 6% weight loss. The corresponding temperature of maximum weight loss rate of 1-OVMT and 5-OVMT in this phase are 280 and 283°C, respectively, which is attributed to OTAB introducing into the VMT galleries. The OTAB with VMT crystal form chemical bonds to improve the thermal

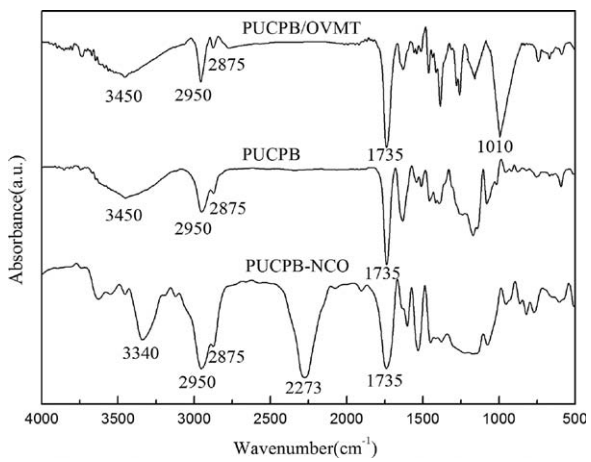

Figure 6. FT-IR spectra of PUCPB and PUCPB/OVMT composites.

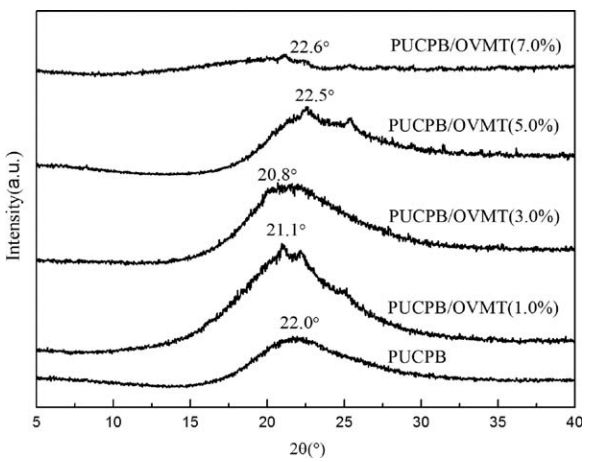

Figure 8. XRD patterns of PUCPB and PUCPB/OVMT composites.

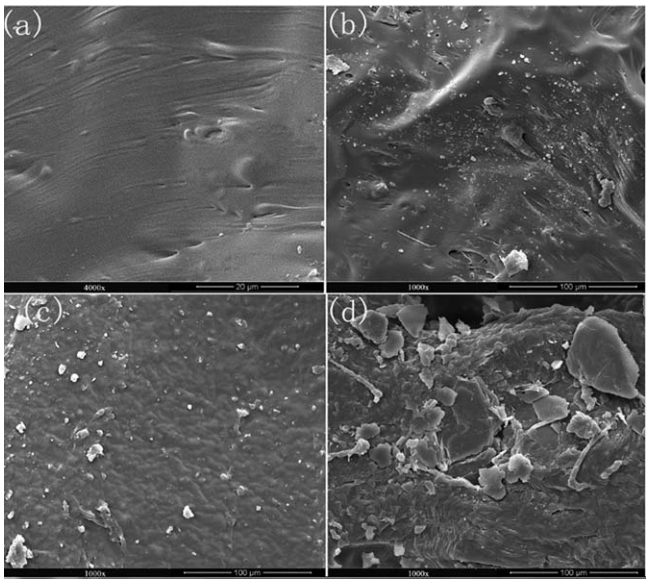

Figure 9. SEM image of (a) PUCPB, (b) PUCPB/OVMT (1.0%), (c) PUCPB/OVMT (5.0%), and (d) PUCPB/OVMT (5.0%).

stability. These results confirm that the OTAB have been intercalated into the galleries of the silicate, the results are matching with XRD analysis.

PUCPB and PUCPB/OVMT Composites

FT-IR Analysis. Figure 6 shows the FT-IR spectra of the prepolymer of PU, PUCPB, and PUCPB/OVMT. The FT-IR spectra are mainly measured by N–H stretching vibrations peaks at 3340–3450 cm^{-1}, the appearance of two peaks at 2950 and 2875 cm^{-1} are related to the methyl ($-CH_3$) and methylene ($-CH_2$) group, respectively. The free –NCO peak stretching at 2273 cm^{-1} in the PU prepolymer proves that system has free –NCO groups and is suitable for the curing reaction. The peak of carbonyl stretching vibration of carbamate stretch at near 1735 cm^{-1}. The Si−O bending vibrations appeared at 1010 cm^{-1} and confirms that the group is introduced into the PU backbone. Besides, the stretching vibration characteristic peaks near the 1635–1690 cm^{-1} attributed to urea base cannot be observed, which proves no reaction between –NCO with water. The appearance of peaks at 3200–3500 and 3500–3600 cm^{-1} is related to the hydrogen-bonded N–H peaks and the free N–H peaks.[25,26]

XRD Analysis of OVMT Dispersion in PCDL and PUCPB/OVMT. Figure 7 shows the XRD patterns of OVMT, PCDL-OVMT (3.0%), and PUCPB/OVMT (3.0%). The layer spacing of OVMT is 2.37 nm, the PCDL is dispersed to 3.0% OVMT using the method of high-speed stirring-ultrasonic dispersion, and the *d*-spacing of PCDL-OVMT (3.0%) increased to 2.92 nm. We can see from the diagram that PCDL diffraction peak is obvious at 20.5°, 21.7°, and 24.6°. After polymerization, a diffraction peak appears at $2\theta = 20.8°$ for the ground PUCPB/OVMT (3.0%). For the composites, the peak at 3° corresponds to the OVMT interlayer platelet spacing almost disappears, indicating the intercalations of PUCPB chains into the OVMT interlayer. The mechanism about formation of the intercalated structure may be attributed to the preintercalation of OTAB and the change in surrounding environment from PCDL to CHDI caused shrinkage of the VMT structure.

Figure 8 shows the XRD patterns of pure PUCPB and PUCPB/OVMT composites. The pure PUCPB showed no more diffraction peaks except for a saddleback at 2θ of around 22.0°. For the composites with OVMT, a wider peak at $2\theta = 20.8°$ could be found in the PUCPB/OVMT(3.0%) composites, which indicates that the PUCPB/OVMT(3.0%) exhibits a structure of more crystallinity than PUCPB and it has a special acting force between PUCPB and OVMT. However, a faint peak could be found when the higher the weight ratio of the OVMT (7.0 wt %) in the PUCPB.

SEM Analysis of PUCPB/OVMT Composites. In Figure 9(a), it is pure PUCPB without joining the OVMT, and the surface of PUCPB is smooth and neat. In Figure 9(b), 1.0 wt % OVMT is distributed in the PUCPB matrix relatively and the layered space is enlarged, but decentralized state is bad. For the case of PUCPB loading of 3.0 wt % OVMT in Figure 9(c), some smaller particles are dispersed and buried in PU. Compared

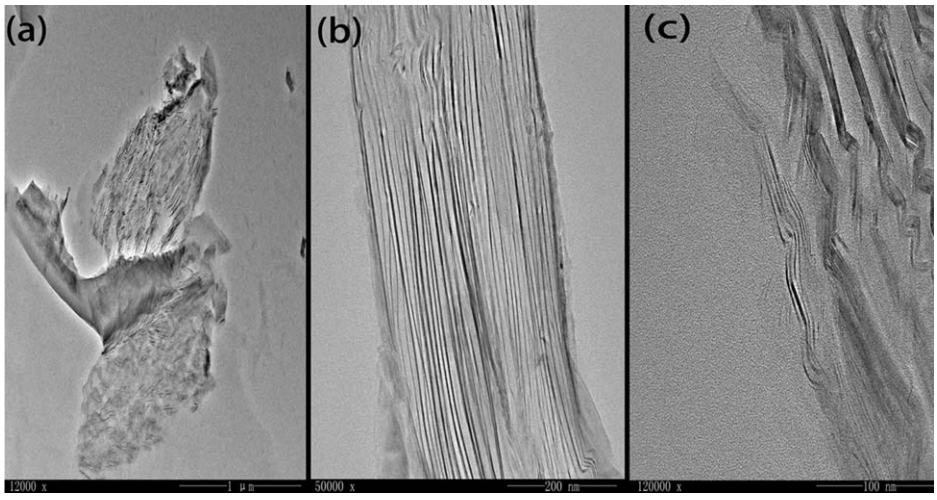

Figure 10. TEM image of PUCPB/OVMT (5.0%).

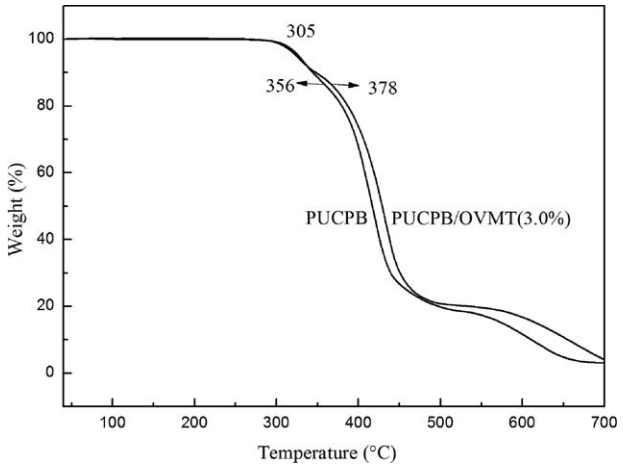

Figure 11. The curves of TGA of PUCPB and PUCPB/OVMT (3.0%) composites.

with Figure 9(b), the adding concentration of modified VMT increased the degree of phase separation of soft segment and hard segment of composites. Better dispersion of OVMT in PUCPB may be attributed to distributive mixing as well as better intrinsic compatibility between OVMT and PCDL. Seen from Figure 9(d), when OVMT content is 5.0%, most of the OVMT is delaminated and disorderly distributed in the matrix phase. The separation degree of soft segment and hard segment of composites increased significantly and it comes out a certain degree of reunion. The outstanding dispersion is one key feature to yield a good composite property. Therefore, it can predict that the composites possess the excellent mechanical properties.

TEM Analysis of PUCPB/OVMT Composites. Figure 10 shows the TEM results of PUCPB/OVMT composites (5.0 wt % OVMT) at 12,000×, 50,000×, and 120,000×, respectively. As shown in Figure 10(a), OVMT is distributed in the PUCPB matrix, and lamellated structure of OVMT is obvious. With higher magnification, as shown in Figure 10(b), the space of interlayer of OVMT is enlarged, which is in keeping with the results of XRD. When the magnification is at 120,000×, not only the insert structure but also the separately distributed OVMT with layer structure is observed.

Thermal and Mechanical Properties of PUCPB and PUCPB/OVMT

Thermal Properties Analysis. The thermal property of the PUCPB and PUCPB/OVMT (3.0%) is evaluated by the TGAs. The typical TGA curves of the PUCPB and PUCPB/OVMT (3.0%) are shown in Figure 11. Generally, the thermal stability of PU is determined by the strength of its weakest bond. It is known that the hard segment is more prone to thermal decomposition than the soft segment in PUCPB. Therefore, CHDI and PCDL are expected to improve the initial decomposition temperature of the PUCPB. The first phase of the initial decomposition temperature of PUCPB/OVMT is 305°C, the weightlessness of PUCPB/OVMT (3.0%) is only 5% at this stage when it is the corresponding temperature of maximum weight loss rate, but weightlessness of pure PU is as high as 10%. The initial decomposition temperature of soft segment is 378°C, and the temperature of maximum weight loss rate of PUCPB/OVMT (3.0%) is 430°C. Based on the temperature corresponding to 20% weight loss, the decomposition temperature of PUCPB/OVMT (3.0%) is increased by about 22°C for pure PUCPB. The movement of PUCPB chains is restricted by hydrogen bonding between ester –CO– groups of PCDL soft segments and –OH groups of OVMT. The nucleation of pure PUCPB occurred and the crystallinity increases by addition of OVMT. A varying weight percentage of OVMT into PUCPB influences the temperature-resistant properties of composites; the temperature resistance of the composites can reach 300°C. In other words, the intercalated OVMT shows a high factor.

Mechanical Properties Analysis. The tensile strength, the increased rates of tensile strength, strain at break, and Shore A hardness are summarized in Table I. Composites showed a very similar trend in mechanical properties compared to pure PUCPB, increasing slightly at first and then decreasing at 5.0 wt % of OVMT. Because the layer spacing of VMT is expanded, PCDL is dispersed into the layers of VMT in the process of intercalating polymerization, which makes it easy to form excellent performance of composites. Low content of OVMT in the dispersion of composites are better, it can improve the performance of composites. With the increase of OVMT, they may be attributed to the difficult dispersibility. They are prone to reunite and form stress concentration and result in the decrease of mechanical properties of composites. On addition of 3.0 wt % OVMT, its tensile strength is 26.8 MPa and strain at break is 443%, increased by 52.3% and 31.5%, respectively, than pure PU. The shore A hardness of PUCPB/OVMT (3.0%) is 76°; the composites shows much less change in hardness, this may be associated with the stripped degree of VMT. The table also shows that the mechanical properties of PUCPB/VMT (3.0%) increased slightly, which is only effected by physical blending of VMT.

Table I. Mechanical Properties of PUCPB and PUCPB/OTAB-VMT Composites

Sample	Tensile strength (MPa)	The increased rates of tensile strength (%)	Strain at break (%)	Shore A hardness (°)
PUCPB	17.6	\	337	67
PUCPB/OVMT (1.0%)	22.3	26.7	393	71
PUCPB/OVMT (3.0%)	26.8	52.3	443	76
PUCPB/OVMT (5.0%)	25.5	44.9	427	74
PUCPB/OVMT (7.0%)	23.1	31.3	406	72
PUCPB/VMT (3.0%)	19.8	12.5	359	69

CONCLUSIONS

Natural VMT is modified by cation exchange with OTAB. The increased interlayer spacing upon cation exchange resulted in better dispersion of the OVMT in PCDL, namely, the better properties of composites. The FT-IR, XRD, TGA, SEM, and tensile strength test are applied to characterize the structure and properties of OVMT and PUCPB/OVMT composites. The results showed that the value of layer spacing of OVMT increased from 0.96 to 2.92 nm compared with the VMT. It can also illustrate that OTAB is indeed inserted into interlayer of VMT by TGA (the decomposition temperature of OTAB is about 285°C) and SEM (OTAB is observed). The –NCO groups of prepolymer and the peak of carbamate and Si–O of composites are characterized by FT-IR. The result showed that the temperature resistance of composites is about 300°C. XRD analysis and SEM micrographs indicated that PUCPB/OVMT (3.0%) composites are highly intercalated and increased the degree of phase separation of soft segment and hard segment. OVMT is distributed in the PUCPB matrix, and the space of interlayer of OVMT is enlarged according to the results of TEM. When the magnification is at 120,000×, not only the insert structure but also the separately distributed OVMT with layer structure is observed. Compared with pure PUCPB, the tensile strength and strain at break of PUCPB/OVMT (3.0%) composite increase about 52.3% and 106%, respectively, due to the function of physical cross-linking of OVMT.

ACKNOWLEDGMENTS

The authors thank the Engineering Research Center of Oilfield Chemistry, Ministry of Education Key for experiment condition support.

REFERENCES

1. Song, M.; Xia, H. S.; Yao, K. J.; Hourston., D. J. *Eur. Polym. J.* **2005**, *41*, 259.
2. Wood, G. The ICI PU Handbook, 2nd ed.; Wiley: New York, **1990**.
3. Wang, Z. M.; John, M.; Zachara, J. Y.; Shang, C.; Jeon, J.; Liu, C. X. *Environ. Sci. Technol.* **2014**, *48*, 7766.
4. ValášKová, M.; Martynková, G. S. *InTechOpen* **2012**; 09.
5. Guggenheim, S.; Adams, J. M.; Bain, D. C.; Bergaya, F.; Bigatti, M. F.; Drits, V. A.; Formoso, M. L. L.; Galán, E.; Kogue, T.; Stanjek, H. *Clays Clay Miner.* **2006**, *54*, 761.
6. Patakfalvi, R.; Dékány, I. *Appl. Clay Sci.* **2004**, *25*, 149.
7. Qian, Y. Q.; Lindsay, C. I.; Macosko, C.; Stein, A. *ACS Appl. Mater. Interfaces* **2011**, *3*, 3709.
8. Park, Y. T.; Qian, Y.; Lindsay, C. I.; Nijs, C.; Camargo, R. E.; Stein, A.; Macosko, C. W. *ACS Appl. Mater. Interfaces* **2013**, *5*, 3054.
9. Tien, Y. I.; Wei, K. H. *Macromolecules* **2001**, *34*, 9045.
10. Marcos, C.; Arango, Y. C.; Rodríguez, I. *Appl. Clay Sci.* **2009**, *42*, 368.
11. Da, K. L.; Hong, B. T.; Ruey, S. T. *Polym. Eng. Sci.* **2007**, *47*, 695.
12. Seo, W. J.; Sung, Y. T.; Han, S. J.; Kim, Y. H.; Ryu, O. H.; Lee, H. S.; Kim, W. N. *J. Appl. Polym. Sci.* **2006**, *101*, 2879.
13. Sun, J. G.; Yang, J. J.; Wu, M. Y.; Zhang, J. *China Syn. Rubber Ind.* **2010**, *33*, 319.
14. Tan, S. Q.; Abraham, T.; Ference, D.; Macosko, C. *Polymer* **2011**, *52*, 2840.
15. Randall, D.; Lee, S. The PUs Book; Wiley: New York: **2002**.
16. Pavlidou, S.; Papaspyrides, C. D. *Prog. Polym. Sci.* **2008**, *33*, 1191.
17. Strankowski, M.; Strankowska, J.; Gazda, M.; Piszczyk, L.; Nowaczyk, G.; Jurga, S. *Exp. Polym. Lett.* **2012**, *6*, 610.
18. Heidarian, M.; Shishesaz, M. R.; Kassiriha, S. M.; Nematollahi, M. *Prog. Org. Coat.* **2010**, *68*, 180.
19. Wu, T. F.; Frydrych, M.; O'Kelly, K. *Biomacromolecules* **2014**, *15*, 2663.
20. Han, X. J.; Huang, Z. M.; Huang, C.; Du, Z. F.; Wang, H.; Wang, J.; He, C. L.; Wu, Q. S. *Polym. Compos.* **2012**, *33*, 2045.
21. Berta, M.; Lindsay, C.; Pans, G.; Camino, G. *Polym. Degrad. Stab.* **2006**, *91*, 1179.
22. Liu, J.; Ma, D. Z. *J. Appl. Polym. Sci.* **2002**, *84*, 2206.
23. Jung, D. H.; Kim, E. Y.; Kang, Y. S.; Kim, B. K. *Colloids Surf. A Physicochem. Eng.* **2010**, *370*, 58.
24. Yao, Z.; Wei, L.; Wei, H.; Weihong, G.; Chifei, W. *Polym. Compos.* **2009**, *10*, 39.
25. Pattanayak, A.; Jana, S. C. *Polymer* **2005**, *46*, 3394.
26. Florian, P.; Jena, K. K.; Allauddin, S.; Narayan, R.; Raju, K. V. S. N. *Ind. Eng. Chem. Res.* **2010**, *49*, 4517.